CONTRAST MEDIA & MOLECULAR IMAGING

Received: 21 September 2011, Revised: 6 July 2012, Accepted: 12 August 2012, Published online in Wiley Online Library: 2012

(wileyonlinelibrary.com) DOI: 10.1002/cmmi.1499

In vitro study of SPIO-labeled human pancreatic cancer cell line BxPC-3

Mingmin Tong[a,b], Fei Xiong[c], Yuzhen Shi[a,b], Song Luo[b], Zhenjuan Liu[b], Zhengcan Wu[b] and Zhongqiu Wang[a]*

ABSTRACT: The survivin gene is highly expressed in pancreatic cancer. The purpose of this study was to design and synthesize functionalized magnetic iron oxide nanoparticles (MNPs) targeting survivin gene for the detection of pancreatic cancer. The pancreatic cancer cell line BxPC-3 with survivin gene expression was selected in this study. The healthy lung fibroblast cell was used as a control. Chitosan-coated MNPs (CS@MNPs) and antisense oligodeoxynucleotide of survivin gene were conjugated to MNPs to give Sur-MNPs. Fourier transform infrared spectroscopy was performed to confirm the conjunction of chitosan. The interactions of MNPs, CS@MNPs, and Sur-MNPs in BxPC-3 cells were observed, recorded and analyzed. The size, morphology, cell uptake, cytotoxicity and stability of those particles were assessed by transmission electron microscope, Prussian blue staining, MTT assay and agarose gel electrophoresis. The magnetic resonance signal intensities of pancreatic cells labeled with CS@MNPs and MNPs, and Sur-MNPs, were compared on T_2-weighted images. The results demonstrated that the level of cellular uptake of CS@MNPs was higher than that of naked MNPs. The Sur-MNPs had a suitable size (12 nm sized core), high stability, no cytotoxicity and good water dispersion. Sur-MNPs did not accumulate in healthy lung fibroblast cells, while being taken up by BxPC-3 cells. The Sur-MNPs in BxPC-3 cells could be visualized on T_2-weighted images, which suggested that Sur-MNPs could be used to detect the expression of survivin gene. Thus, Sur-MNPs may be a potential molecular imaging probe targeting survivin gene for early detection of pancreatic cancer cells. Copyright © 2012 John Wiley & Sons, Ltd.

Keywords: magnetic iron oxide nanoparticles; survivin; pancreatic cancer; magnetic resonance image

1. INTRODUCTION

Pancreatic cancer is one of the most common malignant tumors. Owing to its nonspecific symptoms, by the time of diagnosis, most patients have advanced disease with a poor prognosis (1,2). Early diagnosis of pancreatic cancers may lead to favourable outcomes. Compared with conventional imaging modalities, which are not optimal in early diagnosis, imaging specific molecular markers of pancreatic carcinoma may make early detection feasible. Survivin gene has been shown to be overexpressed in several malignant tumors, including pancreatic cancer, lung cancer and breast cancers (3–6). Based on recent study, more than 75% of pancreatic cancer specimens have been reported to express survivin gene (7). Novel methods in molecular imaging using nanotechnology provide some promise in developing an imaging strategy for early detection of these cancers (8–10). One such nanoparticle is magnetic iron oxide nanoparticle (MNPs, γ-Fe_2O_3), a superparamagnetic iron oxide (SPIO) nanoparticle that can be imaged on T_2-weighted magnetic resonance imaging (MRI) (11,12). When attached to an appropriate carrier, it could serve as a vehicle for tracking protein, antibody and gene biomarkers (13–15). However, there are no studies examining its application as the carrier of survivin gene for magnetic resonance imaging. Chitosan is a polysaccharide acquired from deacetylation of natural chitin (16,17) and can be used as a carrier across the cell membrane. It has been extensively utilized as the coating of the magnetic nanoparticles owing to its nontoxic, biodegradable nature and its function of protecting DNA from DNase degradation. In addition, its paramagnetic effect can be quantified by MRI in a dose-dependent manner (18–20). It has already been reported that a SPIO nanoparticle concentration of 25–50 $\mu g\ ml^{-1}$ in medium could make cell transfection effective (8,21,22).

Survivin gene has been proved to be highly expressed in pancreatic cancer cell line BxPC-3 and its antisense oligodeoxynucleotide (ASODN), complementary to a special sequence of survivin mRNA from 27 to 43 nucleotides, can specifically detect the survivin gene of tumor cells (7,23).

In the current study, we aimed to study the preparation of an MR molecular probe targeting survivin gene and its labeling efficiency of pancreatic cancer cell line BxPC-3. Pancreatic cancer cell line BxPC-3 was used to study the efficacy of labeling and detection *in vitro*. Normal lung fibroblast cell was used as a control.

* *Correspondence to: Z. Wang, Department of Radiology, East Hospital, Tongji University School of Medicine, 150 Jimo Road, Shanghai 200120, People's Republic of China. Email: zhq2001us@yahoo.com*

a *M. Tong, Y. Shi, Z. Wang*
Department of Radiology, East Hospital, Tongji University School of Medicine, 150 Jimo Road, Shanghai 200120, People's Republic of China

b *M. Tong, Y. Shi, S. Luo, Z. Liu, Z. Wu*
Department of Medical Imaging, Jinling Hospital, Nanjing University School of Medicine, 305 East Zhongshan Road, Nanjing 210002, People's Republic of China

c *F. Xiong*
State Key Laboratory of Bioelectronics, Jiangsu Laboratory for Biomaterials and Devices, School of Biological Science and Medical Engineering, Southeast University, Nanjing 210096, People's Republic of China

2. MATERIALS AND METHODS

2.1. Synthesis of Chitosan-Coated MNPs

MNPs were synthesized by chemical coprecipitation of ferrous and ferric chlorides in aqueous solution (24). Chitosan (low molecular, Sigma Aldrich) coated magnetic nanoparticles were synthesized by following steps. Before adding to MNPs, chitosan was dissolved in 0.5% (v/v) acetic acid solution (the molar ratio of glucosamine unit to Fe was 1: 30), following a method described by Ge *et al*. (25). The mixture was stirred continuously for 4 h in the air. Then particles were collected using permanent magnet, washed in deionized water to remove dissociative chitosan, and then diverged in an ultrasonicator. After washing the particles three or four times, the nanoparticles were finally diluted into deionized water; the pH value was adjusted to 5.5.

2.2. Synthesis of Antisense Magnetic Molecular Probe (Labeled as Sur-MNPs)

The antisense oligonucleotide was synthesized by Shanghai Shenggong Biotechnology Co. Ltd (Shanghai, China). The sequence of ASODN was 5′-COOH-CTGAGAAAGGGCTGCCAGTCTCAG-3′. The synthesis of Sur-MNPs was performed using EDC–NHS [1-ethyl-3-(3-dimethyl-amino-propyl)-1-carbo- diimidehydrochloride–*N*-hydroxysuccinimide]. ASODN was activated using EDC–NHS at room temperature for 15 min prior to the synthesis of the probe.

Activated ASODN was then added into CS@MNPs and then the mixture was shaken for 2 h in a swing bed at room temperature. The mixture was then washed three times and ultimately diluted into MES [2-(*N*-morpholino) ethanesulfonic acid hydrate; pH 5.5] for further experiments.

2.3. Characterization

Thermogravimetric analysis (TGA) was carried out using a TGA 2050 thermogravimetric analyzer (TA Instruments, USA). The magnetic property was analyzed using a vibrating sample magnetometer (VSM; Lakeshore 7407, USA) with a saturating field of 1 T. Fourier transform infrared (FTIR) spectroscopy was measured on a Bruker Fourier transform spectrometer (VECTOR22) that used KBr pressed disks. The samples (2.325 mg) were heated from room temperature to 700 °C at a heating rate of 20.00 °C min^{-1} in nitrogen gas. The results of the hydrodynamic size distribution of the nanoparticles were obtained by dynamic light scattering (Beckman, USA). The morphology and size of the sample were characterized by transmission electronmicroscopy (TEM; Jeol, JEM-2100, Japan).

2.4. Cell Culture

2.4.1. *Cellular uptake of MNPs*

BxPC-3 was obtained from Origin Bioscience Inc. (Nanjing city, Jiangsu Province, PRC). The cells were cultured in RPMI 1640 medium containing 10% fetal calf serum and then incubated at 37 °C in 5% CO_2 atmosphere. The growth medium was changed every 2 days. To label the cells, the BxPC-3 cell line was seeded at a density of 1×10^5 cell per well in a six-well plate.When BxPC-3 cells confluenced to 80%, a fresh medium with nanoparticles at a concentration of 25 μg ml^{-1} replaced the previous one. The cells were then cultured for another 24 h and washed with phosphate buffered saline (PBS; pH 7.4) three times to remove loosely attached and free particles in the medium.

2.4.2. *In vitro* cell viability and cytotoxicity studies

The cell viability testing of γ-Fe_2O_3 nanoparticles and CS@MNPs was determined by the viability of BxPC-3, using healthy lung fibroblast cell line WI-38 as a contrast group. After incubation with above two nanoparticles separately, 80 μl of MTT (3,4, 5-dimethyl thiazolyl-2,5-diphenylterazoium, BIO) dye solution (5 mg ml^{-1} in medium) was added to each well for further experiments. The medium was completely removed, after incubation at 37 °C under a 5% CO_2 atmosphere for 4 h. Meanwhile formazan crystals were dissolved in 800 μl of dimethyl sulfoxide for 15 min. Absorbance of the solution was measured at 570 nm on a microplate reader (model 680, Bio-RAD, USA). The result was calculated referenced with control cells.

2.4.3. *Qualitative and quantitative analysis of cellular uptake of MNPs*

A Prussian blue staining assay was used to research the cellular uptake of magnetic nanoparticles under an optical microscopy. The labeled cells were washed three times with PBS and then fixed in 4% glutaraldehyde solution subsequently for 20 min. For Prussian blue staining, the labeled cells were incubated for 30 min in 4% potassium ferrocyanide in 4% HCl (freshly prepared) and counterstained with Nuclear Fast Red.

To measure the amount of intracellular SPIO, the labeled cells were digested in HCl (30% v/v) at 60 °C for 2 h, and the solution was treated in the way of phenanthroline. The iron concentration was measured using the *o*-phenanthroline method.

2.4.4. *Transmission electron microscopy*

After being labeled with γ-Fe_2O_3 nanoparticles and Sur-MNPs, the cells were washed three times with distilled water and then fixed with 1% osmic acid for 2 h at 4 °C. Subsequently, they were dehydrated with a series of alcohol concentrations, treated with propylene epoxide, and embedded with epoxy resin finally. The cells were then cut into ultra-thin sections and observed under a TEM (Jeol, JEM-1011).

2.4.5. *The stability of Sur-MNPs by agarose gel electrophoresis*

To prepare a 2% agarose gel solution, 0.6 g of agarose gel was added to a 30 ml TE buffer after heating, and 1 μl of Gel Red (Boitium) was added afterwards. The solution was powered into mode, and a comb was inserted subsequently. It was then cooled at room temperature for about 30 min. DNA/MNPs in different ratios was prepared in this assay. ASODN and the samples of Sur-MNPs were added to the well and electrophoresed at 80 V for 20 min. Then, gel was observed with a gel spectrophotometer.

2.4.6. *In vitro* MR imaging

MR signal intensity was observed on a 1.5 T MR scanner (Siemens Healthcare; Erlangen, Germany). Pancreatic cancer cells were cultured and prepared before MR imaging. The suspension of cells (~1×10^5) with 1% agarose in 1.5 ml Eppendorf tubes was scanned under an MR scanner using a surface coil. Scanning parameter was as follows: repetition time (*TR*) 2500 ms; multi-echo time from 22 to 352 ms; contrast 16; slice thickness 5 mm; field of view 250 mm. Multi-echo T_2 images were obtained for calculation of T_2 values using workplace software (Syngo MMWP VE36A). Circular regions of interest of 33 mm^2 were drawn on the T_2 map image to obtain the T_2

value of each sample. Distilled water and the unlabeled cells served as the control groups. The results were recorded as means ± standard.

3. RESULTS

3.1. Characterizations of Magnetic Nanoparticles

TGA was carried out to confirm the coating of chitosan. The results showed that chitosan makes up about 4% of the CS@MNPs, which was lower than that in Shi's data (26). In Shi's work, carboxymethylated chitosan linked to the SPIO modified with (3-aminopropyl) rimethoxysilane via EDC–NHS was presented. Figure 1 shows the FTIR spectra of Chitosan, MNPs, and CS@MNPs. The characteristic absorption bands of the Fe–O stretch are at 588 and 632 cm^{-1} in CS@MNPs. Chitosan appeared at 1646 cm^{-1} (amide I), 1618 cm^{-1} (amide II) and 1400 cm^{-1} (amide III).

The size and morphology of the individual CS@MNPs were about 12 nm based on the TEM images (Figs 2 and 3), while the hydrodynamic size distribution of the particles was about 129 nm. The obvious curve of VSM shown in Fig. 4 and Table 1 demonstrates that both MNPs have the property of superparamagnetism. Furthermore, there was no change of superparamagnetic property after coating. The saturation magnetization (M_s), remnant magnetization (M_r) and coercivity (H_c) are shown in Table 1. The reduction of Ms after modifying with chitosan can be explained as the presence of nonmagnetic surfactant molecules.

3.2. *In Vitro* Cell Viability and Cytotoxicity Studies

MTT assay was utilized for cell viability evaluation to determine biomaterial toxicity of cells. The viability of BxPC-3 cells and lung fibroblasts was measured by MTT assay after culturing for 24 h. Figure 5 displays a dose-dependent reduction in MTT absorbance for cells treated with CS@MNPs and MNPs. The data reveal

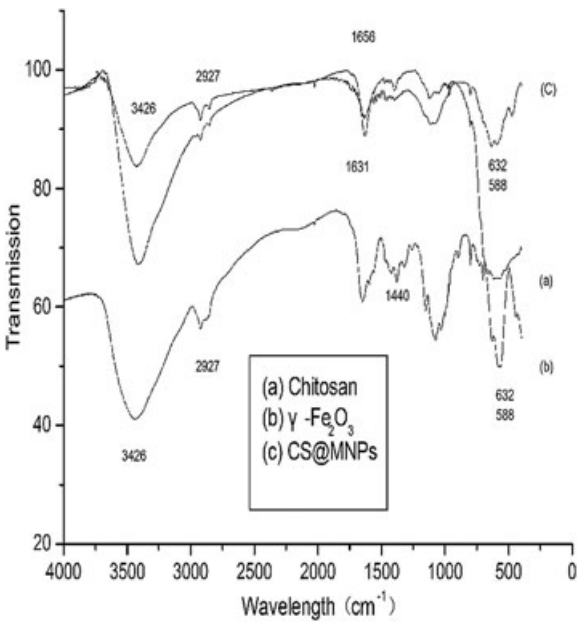

Figure 1. IR spectrum of magnetic iron oxide nanoparticles (MNPs), chitosan (CS) and chitosan modified magnetic nanoparticles (CS@MNPs).

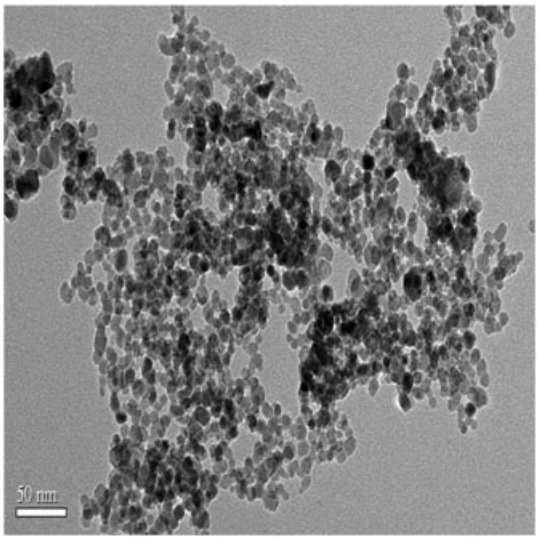

Figure 2. Transmission electronmicroscopy (TEM) distribution image of CS@MNPs.

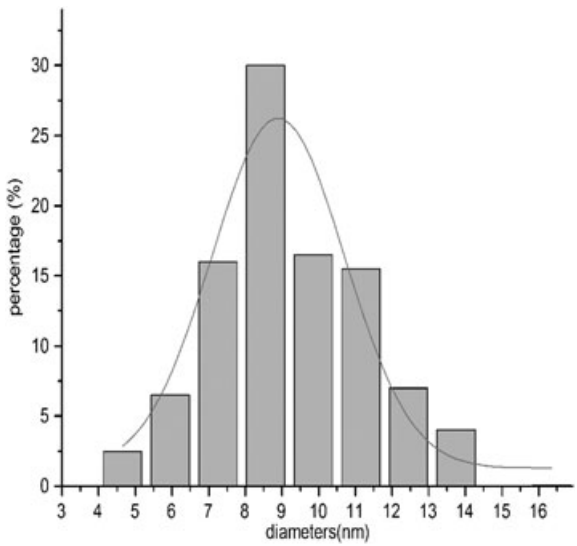

Figure 3. Size distribution image of CS@MNPs.

that the nanoparticles presented low cytotoxicity after coating with chitosan. Additionally, they had a higher inhibition ratio to cancer cells than normal cells.

3.3. Qualitative Studies

Many blue particles could be seen when cells were incubated with CS@MNPs and Sur-MNPs, less with γ-Fe_2O_3, while none were observed in unlabeled cells (Fig. 6). The highest uptake amount of the three groups was for Sur-MNPs (18.24 ± 0.79 pg); the group of γ-Fe_2O_3 was the lowest (9.32 ± 0.21 pg). It is possible that the antisense oligonucleotide, when combined with the mRNA, cuts down the backflow of MNPs (Fig. 7). As shown in Fig. 8, TEM studies of BxPC-3 cells treated with CS@MNPs and Sur-MNPs revealed that most nanoparticles were endocytosed and accumulated in cytoplasm.

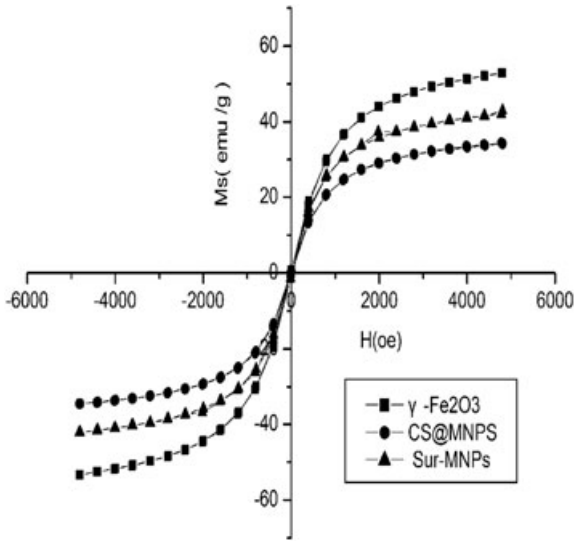

Figure 4. Vibrating sample magnetometry (VSM) of CS@MNPs, CS@MNPs and magnetic targeted probes (Sur-MNPs).

Table 1. Magnetic properties and δ-potential of MNPs, CS@MNPs and Sur-MNPs

Samples	M_s (emu g^{-1})	H_c (Oe)	δ-Potential (mV)
MNPs	52. 7374	9.0	—
CS@MNPs	34.1494	8.53	21.15 ± 3.09
Sur-MNPs	42.093	14	7.76

M_s, Saturation magnetization; H_c, coercivity.

3.4. The Stability of Sur-MNPs by Agarose Gel Electrophoresis

As can be seen from Fig. 9, at various rates, the ASODN can combine with the MNPs, and the amount of free ASODN in the complex was negligible. After linking to the MNPs, the mobility of ASODN was restricted. It was most obviously shown at the ratio of 1: 100 in Fig. 9.

3.5. Magnetic Resonance Imaging

The mean T_2 relaxation times of unlabeled cells, cells labeled with MNPs, CS@MNPs, and Sur-MNPs were 331.5 ± 18.3, 219.5 ± 21.8, 218.0 ± 17.3 and 171.7 ± 32.5 ms, respectively. T_2-Weighted imaging of the samples is shown in Fig. 10.

4. DISCUSSION

Molecular imaging emerges as a promising and reliable technique due to recent advances in biotechnology and medical imaging (7,12). Targeting specific markers with molecular imaging probes for early detection of tumors and monitoring personalized therapeutics has great potential for revolutionizing cancer care in the next few decades. Appropriate selection of the marker and development of an optimal molecular imaging probe is the key in these endeavors. Developing an optimal probe is challenging as it requires probes with low cytotoxicty that are easily biodegradable and sufficiently stable that a strong imaging signal can be obtained. MRI, SPECT, PET and optical imaging have all been used to image these probes in recent years.

In this study, we selected survivin gene as the target marker and chitosan-coated magnetic iron oxide particles as the imaging probe for detection of pancreatic cancer (27,28). Magnetic nanoparticles have been used as contrast agents for liver and lymph node imaging, and ever greater interest has been focused on their use as specific molecular probe for tumors (8,14). Yang *et al*. designed a nanoparticle probe targeted urokinase plasminogen activator (cellular receptor) for early diagnosis and monitoring of breast cancer and pancreatic cancer with MR imaging (29). Peng *et al*. developed a molecular beacon-based molecular imaging approach for detecting specific tumor genes *in vitro* (30). Since survivin gene is expressed in the cytoplasm rather than the cell membrane, we needed to choose a probe that could traverse the cell membrane intracytoplasmic in location with no expression on the cell membrane (3,31). We selected chitosan to modify the MNPs and as the carrier of DNA owing to the ablity of chitosan to enter cells (31). Chitosan is rich in amino groups that can be conjoined to the DNA modified with carboxy with the help of EDC–NHS (32). We linked chitosan to

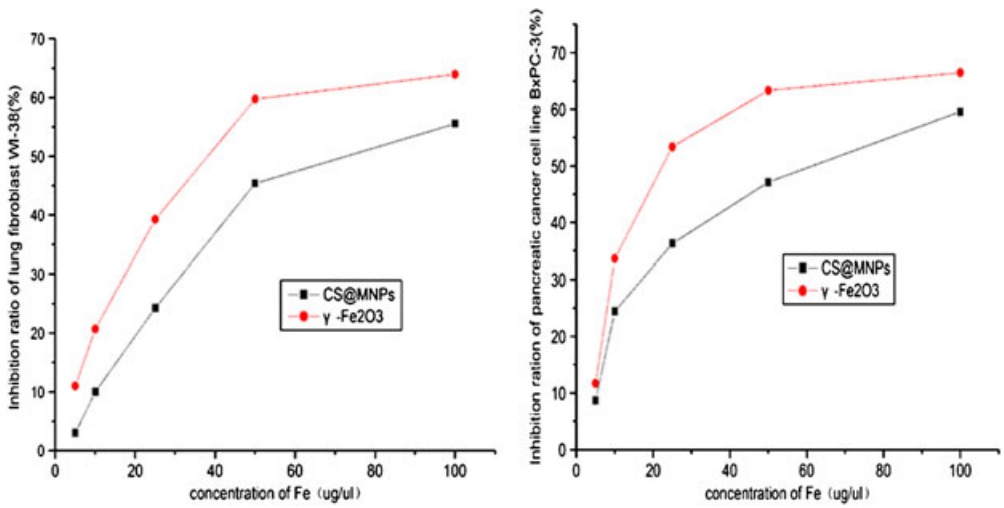

Figure 5. The MTT result of MNPs with BxPC-3 cells and the result of MNPs with lung fibroblasts.

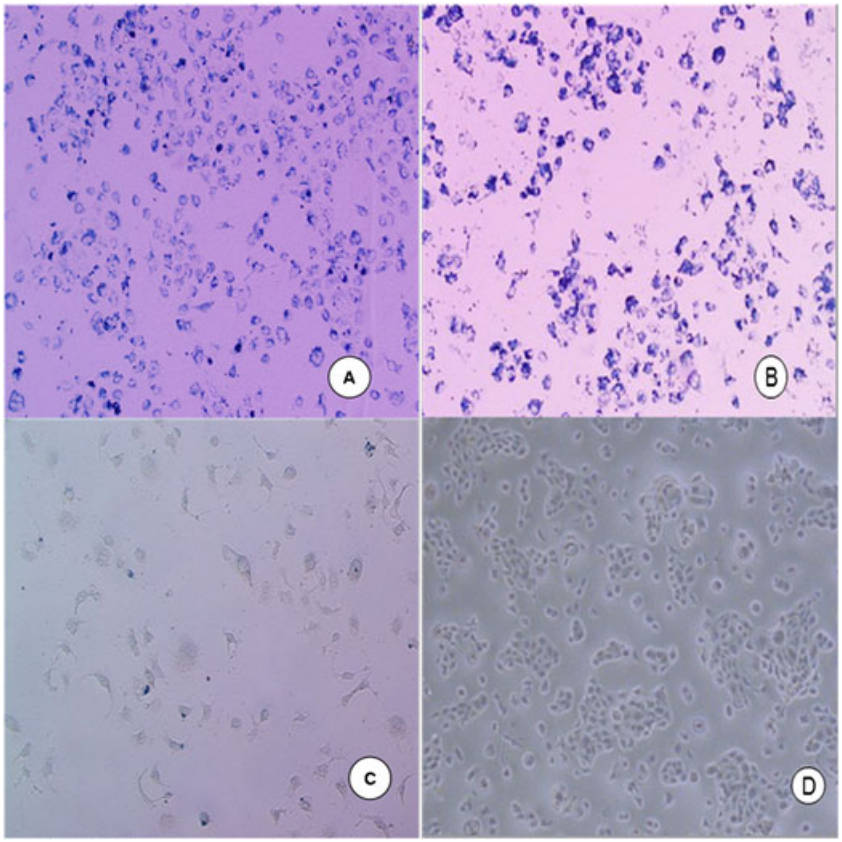

Figure 6. Prussian blue staining of labeled BxPC-3 cells revealed uptake after 24 h of incubation. Cells labeled with CS@MNPs (A), Sur-MNPs (B), MNPs (C) and unlabeled control cells (D).

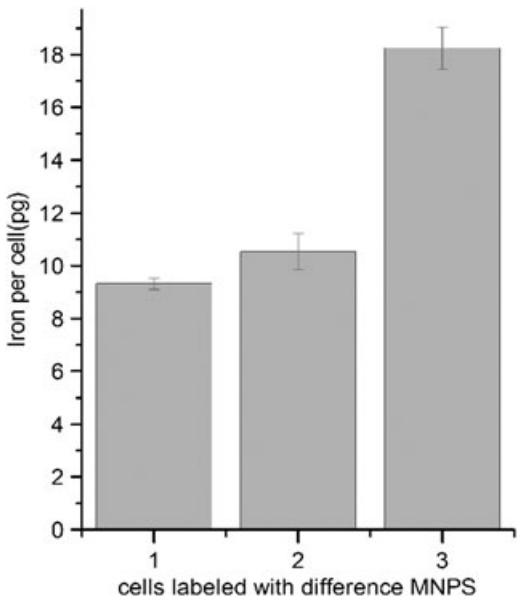

Figure 7. Determination of the various MNPs for interaction with BxPC-3 cells for 24 h. Cells labeled with MNPs (1), CS@MNPs (2) and Sur-MNPs (3). Results are shown as means ± SD.

the surface of MNPs successfully, which enhanced the the biocompatibility of the complex and provided the amino group for the antisense oligonucleotide. Furthermore, we paired the chitosan-coated MNPs complex with antisense oligonucleotide complementary to the survivin mRNA in pancreatic cancer line BxPC-3.

The results of TGA and FTIR in our study proved that the nanoparticles can be successfully modified with chitosan, and the magnetic property of magnetic nanoparticles was not altered after coating. The uniform core size of CS@MNPs was 12 nm, which is obviously smaller than the maximum size of 50 nm prescribed for a molecular probe (33,34). Hence we conclude that the magnetic nanoparticles that we designed and produced are suitable for imaging *in vitro* and *in vivo* on a molecular medical level.

Our MTT result revealed that the vitality of BxPC-3 cells was enhanced when cultured with chitosan-modifying MNPs compared with the cells cultured with unmodified MNPs, even at an iron concentration of 100 $\mu g\,ml^{-1}$, which resulted in better transfection efficiency. That confimed that MNPs will be more prone to enter the BxPC-3 cell after modification with chitosan. The results of BxPC-3 cells treated with Sur-MNPs proved that most nanoparticles were endocytosed and accumulated in cytoplasm by TEM. The T_2* effect of the paramagnetic Sur-MNP was detected on T_2-weighted images. A possible reason for this is that the cancer cells took in more magnetic nanoparticles than the normal cells, as Vigor *et al*. reported (35).

Our magnetic molecular probe was developed via linking antisense oligonucleotide to the surface of CS@MNPs, involving the interaction of amino and carboxyl groups, which was more stable than other combination methods, such as electrostatic interaction and antigen–antibody reaction (8,21). The agarose

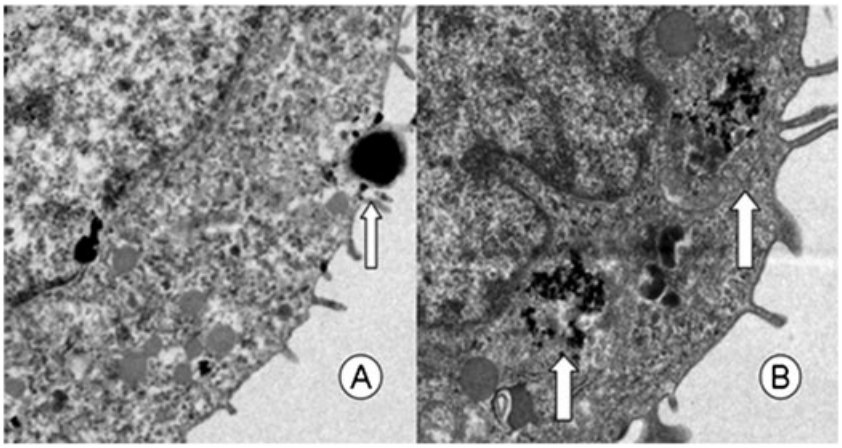

Figure 8. TEM images of BxPC-3 cells incubated with MNPs (A) and Sur-MNPs (B), for 24 h (white arrow points to the particles).

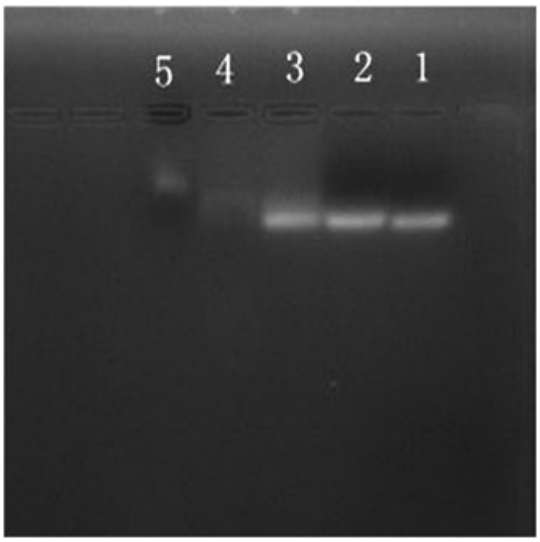

Figure 9. The electrophoresis results of antisense oligonucleotide of survivin and Sur-MNPs at different ratios. 1, Pure survivin antisense DNA; 2–5, sample of Sur-MNPs at ratios of 1: 10, 1: 30, 1: 50 and 1: 100.

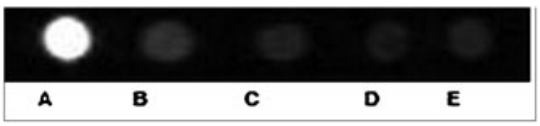

Figure 10. T_2-weighted imaging of the samples. (A) Water; (B) unlabeled cells (2×10^5 cells ml^{-1}); (C) cells labeled with MNPs; (D) cells labeled with Sur-MNPs; (E) cells labeled with CS@MNPs. From the figure, we get that (C)–(E) showed lower signals than (A) and (B); (D) and (E) were lower than (C); (A) had the highest signal of all. The singal of (D) was the lowest.

gel electrophoresis demonstrated that the mobility of the DNA was retarded in direct correlation to increasing proportions of CS@MNPs, perhaps because the negative charge of DNA was neutralized by the positive charge on MNPs. The mobility of the DNA was the slowest at the rate of 1: 100 (Fig 9).

To determine whether the labeled cells obtained the property of the magnetic probe, we imaged them using a 1.5 T MR scanner. The Sur-MNPs labeled cells showed low signal owing to the T_2-weighting effect, indicating that Sur-MNPs may be a good negative molecular imagine contrast agent for detection of some malignant tumors.

Our research results prove that survivin gene of pancreatic cancer could be detected by Sur-MNPs, thereby suggesting the benefit of our approach in detection of pancreatic cancer. The potential translational and clinical application of this technique is immense and may pave way for early detection of pancreatic cancer and management. Many challenges remain before this technique can be applied to a clinical setting. These include overcoming the uptake of nanoparticles by the cells of the reticuloendothelial system (21,27), and delivery of sufficient amount of nanopaticles to the tumor tissue for MRI visualization.

5. CONCLUSIONS

In summary, we have developed a survivin gene-targeted magnetic nanoprobe – Sur-MNPs. It was successfully synthesized, had a suitable size (12 nm sized core) and stable link, and dispersed well in water, preventing aggregation. The Sur-MNPs are biocompatible and biodegradable. This novel magnetic molecular probe can cause reduction of the T_2 relaxation time on MR molecular imaging. The Sur-MNPs allow the selective delivery of nanoparticles into primary pancreatic cancer cells (BxPC-3). Sur-MNPs can specifically accumulate in pancreatic cancer cells with surviving gene expression, holding great promise in imaging pancreatic cancer and monitoring therapy (23). Further studies to evaluate the selective uptake of Sur-MNPs in pancreatic cancer xenografts *in vivo* are currently underway.

Acknowledgments

This study was sponsored by the Natural Science Foundation Project of China (nos 30870689, 81071195, 81271630 and 81001412) and the Natural Science Foundation Project of Jiangsu Province, China (BK2008325). We thank Dr Raghu Vikram from Section of Body Imaging, Department of Diagnostic Radiology, the University of Texas MD Anderson Cancer Center. We also thank Professor Chun Li from the Department of Experimental Diagnostic Imaging, the University of Texas MD Anderson Cancer Center for his scientific revision and comments

REFERENCES

1. Shami VM, Mahajan A, Loch MM, Stella AC, Northup PG, White GE, Brock AS, Srinivasan I, de Lange EE, Kahaleh M. Comparison between endoscopic ultrasound and magnetic resonance imaging for the staging of pancreatic cancer. Pancreas 2011; 40: 567–570; DOI: 10.1097/MPA.0b013e3182153b8c
2. Holzapfel K, Reiser-Erkan C, Fingerle AA, Erkan M, Eiber MJ, Rummeny EJ, Friess H, Kleeff J, Gaa J. Comparison of diffusion-weighted MR imaging and multidetector-row CT in the detection of liver metastases in patients operated for pancreatic cancer. Abdom Imag 2011; 36: 179–184; DOI: 10.1007/s00261-010-9633-5
3. Jiang C, Tan T, Yi XP, Shen H, Li YX. Lentivirus-mediated shRNA targeting XIAP and survivin inhibit SW1990 pancreatic cancer cell proliferation in vitro and in vivo. Mol Med Rep 2011; 4: 667–674; DOI: 10.3892/mmr.2011.472
4. Glienke W, Maute L, Wicht J, Bergmann L. The dual PI3K/mTOR inhibitor NVP-BGT226 induces cell cycle arrest and regulates Survivin gene expression in human pancreatic cancer cell lines. Tumour Biol 2011; DOI: 10.1007/s13277-011-0290-2
5. Glienke W, Maute L, Wicht J, Bergmann L. Curcumin inhibits constitutive STAT3 phosphorylation in human pancreatic cancer cell lines and downregulation of survivin/BIRC5 gene expression. Cancer Invest 2010; 28: 166–171; DOI: 10.3109/07357900903287006
6. Xue Y, An R, Zhang D, Zhao J, Wang X, Yang L, He D. Detection of survivin expression in cervical cancer cells using molecular beacon imaging: new strategy for the diagnosis of cervical cancer. Eur J Obstet Gynecol Reprod Biol 2011; 159: 204–208; DOI: 10.1016/j.ejogrb.2011.06.038
7. Yang L, Cao Z, Lin Y, Wood WC, Staley CA. Molecular beacon imaging of tumor marker gene expression in pancreatic cancer cells. Cancer Biol Ther 2005; 4: 561–570; DOI: 1670 [pii]
8. Xu H, Aguilar ZP, Yang L, Kuang M, Duan H, Xiong Y, Wei H, Wang A. Antibody conjugated magnetic iron oxide nanoparticles for cancer cell separation in fresh whole blood. Biomaterials 2011; 32: 9758–9765; DOI: 10.1016/j.biomaterials.2011.08.076
9. Liao Z, Wang H, Lv R, Zhao P, Sun X, Wang S, Su W, Niu R, Chang J. Polymeric liposomes-coated superparamagnetic iron oxide nanoparticles as contrast agent for targeted magnetic resonance imaging of cancer cells. Langmuir 2011; DOI: 10.1021/la1050157
10. Alexiou C, Schmid RJ, Jurgons R, Kremer M, Wanner G, Bergemann C, Huenges E, Nawroth T, Arnold W, Parak FG. Targeting cancer cells: magnetic nanoparticles as drug carriers. Eur Biophys J 2006; 35: 446–450; DOI: 10.1007/s00249-006-0042-1
11. Maeng JH, Lee DH, Jung KH, Bae YH, Park IS, Jeong S, Jeon YS, Shim CK, Kim W, Kim J, Lee J, Lee YM, Kim JH, Kim WH, Hong SS. Multifunctional doxorubicin loaded superparamagnetic iron oxide nanoparticles for chemotherapy and magnetic resonance imaging in liver cancer. Biomaterials 2010; 31: 4995–5006; DOI: 10.1016/j.biomaterials.2010.02.068
12. Li Z, Kawashita M, Araki N, Mitsumori M, Hiraoka M, Doi M. Preparation of magnetic iron oxide nanoparticles for hyperthermia of cancer in a FeCl-NaNO-NaOH aqueous system. J Biomater Applic 2011; 25: 643–661; DOI: 10.1177/0885328209351136
13. Haud N, Kara F, Diekmann S, Henneke M, Willer JR, Hillwig MS, Gregg RG, Macintosh GC, Gartner J, Alia A, Hurlstone AF. rnaset2 Mutant zebrafish model familial cystic leukoencephalopathy and reveal a role for RNase T2 in degrading ribosomal RNA. Proc Natl Acad Sci USA 2011; 108: 1099–1103; DOI: 10.1073/pnas.1009811107
14. Bae KH, Lee K, Kim C, Park TG. Surface functionalized hollow manganese oxide nanoparticles for cancer targeted siRNA delivery and magnetic resonance imaging. Biomaterials 2011; 32: 176–184; DOI: 10.1016/j.biomaterials.2010.09.039
15. Lavergne E, Hendaoui I, Coulouarn C, Ribault C, Leseur J, Eliat PA, Mebarki S, Corlu A, Clement B, Musso O. Blocking Wnt signaling by SFRP-like molecules inhibits in vivo cell proliferation and tumor growth in cells carrying active beta-catenin. Oncogene 2011; 30: 423–433; DOI: 10.1038/onc.2010.432
16. Zhang Y, Zhang MQ. Cell growth and function on calcium phosphate reinforced chitosan scaffolds. J Mater Sci Mater Med 2004; 15: 255–260; DOI: 10.1023/B: JMSM.0000015485.94665.25
17. Peluso G, Petillo O, Ranieri M, Santin M, Ambrosio L, Calabro D, Avallone B, Balsamo G. Chitosan-mediated stimulation of macrophage function. Biomaterials 1994; 15: 1215–1220; DOI: 10.1016/0142-9612(94)90272-0
18. Zhou Q, Dergunov SA, Zhang Y, Li X, Mu Q, Zhang Q, Jiang G, Pinkhassik E, Yan B. Safety profile and cellular uptake of biotemplated nanocapsules with nanometre-thin walls. Nanoscale 2011; 3: 2576–2582; DOI: 10.1039/c1nr10311c
19. Zhang Y, Chen J, Pan Y, Zhao J, Ren L, Liao M, Hu Z, Kong L, Wang J. A novel PEGylation of chitosan nanoparticles for gene delivery. Biotechnol Appl Biochem 2007; 46: 197–204; DOI: 10.1042/BA20060163
20. Zhang LW, Monteiro-Riviere NA. Mechanisms of quantum dot nanoparticle cellular uptake. Toxicol Sci 2009; 110: 138–155; DOI: 10.1093/toxsci/kfp087
21. Nam T, Park S, Lee SY, Park K, Choi K, Song IC, Han MH, Leary JJ, Yuk SA, Kwon IC, Kim K, Jeong SY. Tumor targeting chitosan nanoparticles for dual-modality optical/MR cancer imaging. Bioconjug Chem 2010; 21: 578–582; DOI: 10.1021/bc900408z
22. Wen M, Li B, Ouyang Y, Luo Y, Li S. Preparation and quality test of superparamagnetic iron oxide labeled antisense oligodeoxynucleotide probe: a preliminary study. Ann Biomed Eng 2009; 37: 1240–1250; DOI: 10.1007/s10439-009-9683-4
23. Henry SP, Giclas PC, Leeds J, Pangburn M, Auletta C, Levin AA, Kornbrust DJ. Activation of the alternative pathway of complement by a phosphorothioate oligonucleotide: potential mechanism of action. J Pharmacol Exp Ther 1997; 281: 810–816.
24. Zhang S, Bian Z, Gu C, Zhang Y, He S, Gu N, Zhang J. Preparation of anti-human cardiac troponin I immunomagnetic nanoparticles and biological activity assays. Colloids Surf B Biointerfaces 2007; 55: 143–148; DOI: 10.1016/j.colsurfb.2006.11.041
25. Ge Y, Zhang Y, Xia J, Ma M, He S, Nie F, Gu N. Effect of surface charge and agglomerate degree of magnetic iron oxide nanoparticles on KB cellular uptake in vitro. Colloids Surf B Biointerfaces 2009; 73: 294–301; DOI: 10.1016/j.colsurfb.2009.05.031
26. Shi ZL, Neoh KG, Kang ET, Shuter B, Wang S-C, Poh C, Wang W. (Carboxymethyl)chitosan-modified superparamagnetic iron oxide nanoparticles for magnetic resonance imaging of stem cells. ACS Appl Mater Interfaces 2009; 1: 328–335; DOI: 10.1021/am8000538
27. Shen YM, Yang XC, Song ML, Qin CH, Yang C, Sun YH. Growth inhibition induced by short hairpin RNA to silence survivin gene in human pancreatic cancer cells. Hepatobiliary Pancreat Dis Int 2010; 9: 69–77; DOI: 1322 [pii]
28. Tsuji N, Asanuma K, Kobayashi D, Yagihashi A, Watanabe N. Introduction of a survivin gene-specific small inhibitory RNA inhibits growth of pancreatic cancer cells. Anticancer Res 2005; 25: 3967–3972.
29. Yang L, Mao H, Cao Z, Wang YA, Peng X, Wang X, Sajja HK, Wang L, Duan H, Ni C, Staley CA, Wood WC, Gao X, Nie S. Molecular imaging of pancreatic cancer in an animal model using targeted multifunctional nanoparticles. Gastroenterology 2009; 136: 1514–1525 e1512; DOI: 10.1053/j.gastro.2009.01.006
30. Peng XH, Cao ZH, Xia JT, Carlson GW, Lewis MM, Wood WC, Yang L. Real-time detection of gene expression in cancer cells using molecular beacon imaging: new strategies for cancer research. Cancer Res 2005; 65: 1909–1917; DOI: 10.1158/0008-5472.CAN-04-3196
31. Bowman K, Leong KW. Chitosan nanoparticles for oral drug and gene delivery. Int J Nanomed 2006; 1: 117–128.
32. Franca EF, Freitas LC, Lins RD. Chitosan molecular structure as a function of N-acetylation. Biopolymers 2011; 95: 448–460; DOI: 10.1002/bip.21602
33. Huang J, Bu L, Xie J, Chen K, Cheng Z, Li X, Chen X. Effects of nanoparticle size on cellular uptake and liver MRI with polyvinylpyrrolidone-coated iron oxide nanoparticles. ACS Nano 2010; 4: 7151–7160; DOI: 10.1021/nn101643u
34. Norek M, Kampert E, Zeitler U, Peters JA. Tuning of the size of Dy2O3 nanoparticles for optimal performance as an MRI contrast agent. J Am Chem Soc 2008; 130: 5335–5340; DOI: 10.1021/ja711492y
35. Vigor KL, Kyrtatos PG, Minogue S, Al-Jamal KT, Kogelberg H, Tolner B, Kostarelos K, Begent RH, Pankhurst QA, Lythgoe MF, Chester KA. Nanoparticles functionalized with recombinant single chain Fv antibody fragments (scFv) for the magnetic resonance imaging of cancer cells. Biomaterials 2010; 31: 1307–1315; DOI: 10.1016/j.biomaterials.2009.10.036